Chapter 5

Kinematics of Low Mass X-Ray Binaries and Millisecond Pulsars

5.1 Introduction

The first binary pulsar PSR B1913+16 was discovered in the year 1974 by Hulse & Taylor (Hulse & Taylor 1975). Many attempts were made to explain the nature of this pulsar, which had a relatively short period ($\sim$ 59 msec) and a low magnetic field (a few times 10^{10} Gauss). Srinivasan & van den Heuvel (1982) explained this combination of short rotational period and low magnetic field in terms of it being recycled in a binary system. When the first millisecond pulsar was discovered in 1982 (Backer *etal.* 1982) the anomalous combination of ultra short period and very low magnetic field led several people to suggest that this too was a recycled pulsar from a binary system (Radhakrishnan & Srinivasan 1982; Alpar *et al.* 1982; Fabian *et al.* 1982).

Very soon, it mas understood that if a neutron star had to be spun up to periods of a millisecond or so, it has to accrete about $0.1M_\odot$, which implied that the mass transfer must last for at least 10 Myr even at the maximum possible Eddington rate. In binary systems with a neutron star and a massive star the mass transfer occurs on the thermal time scale of the massive star. Therefore even if the neutron star accretes matter at Eddington rate it can not accrete enough matter to get spun-up to millisecond periods. However, in a binary system where the companion is less massive than the neutron star the mass transfer can last for such long time scales, since the mass is transferred on the nuclear time scale (see for example Joss & Rappaport 1983). Hence, it was suggested that Low Mass X-Ray Binaries may be the progenitors of millisecond pulsars. However, this has been debated in the literature, with the alternative mechanism that millisecond pulsars can be produced by Accretion Induced White dwarf Collapse (AIWC). If the former mechanism is true, one expects the kinematic properties of LMXBs to be identical to those of millisecond pulsars. This chapter describes a study of the kinematic properties of these two populations.

Many assumptions have been made to do this simulation, and Section 2 describes all of them. The procedure which we have followed to do the simulation and the results of the simulation are described in section **3.** The discussions, followed by a set of conclusions are described in section4.

5.2 Assumptions

Most of the assumptions are pretty much similar to the assumptions listed in chapter **3.** A large number of binaries were generated with initial primary masses in the range $10 \leq (M_1^\circ/M_\odot) \leq 20$, with the distribution proportional to $M^{-2.7}$. The initial mass ratios are generated (with a uniform probability) in the range $0.02 \leq q \leq 0.15$. The binaries with companion masses greater than $1.5 M_\odot$ are not considered for the simulation.

It has been assumed that during the primary overflow the binary necessarily goes through a spiral-in phase, and the whole of the lost orbital energy is used to expell out the envelope (*i.e.*, radiative losses are negligible). The change in the orbital semimajor axis is given by the following equation (Webbink 1984; Bhattacharya & van den Heuvel 1991),

$$\frac{a}{a_\circ} = \left(\frac{M_2 M_{1c}}{M_{1c} + M_{1e}}\right)\left(\frac{1}{M_2 + 2M_{2e}/\lambda r_L}\right) \tag{5.1}$$

where a and a, are the final and initial semimajor axes, M_2 is the mass of the low mass companion, M_{1e} and M_{1c} are the mass of the envelope and the core of the massive primary star, $(a_\circ r_L)$ is the Roche-lobe radius of the primary star, and λ is the weighting factor (< 1) for the gravitational binding energy of the core and the envelope of the star. For this simulation, the value of λ has been assumed to be 0.5.

The magnitude of the velocity of the centre of mass of the binary system (if it survives) after the supernova explosion is given by,

$$V_{\rm cm} = \left[\frac{(M_{1f}v_1 - M_2 v_2)^2 + M_{1f}^2 v_k^2 + 2M_{1f}v_k(M_{1f}v_1 - M_2 V_2)\cos\theta}{(M_{1f} + M_2)^2}\right]^{1/2} \tag{5.2}$$

where M_{1f} is the primary mass after the explosion, v_1 and v_2 are the pre-explosion orbital velocities of the two masses, v_k is the magnitude of the asymmetric kick velocity, and θ is the angle between $\vec{v}_2$ and $\vec{v}_k$. The direction of this centre of mass velocity in the Galaxy was assumed to be completely random.

5.2.1 The gravitational potential function of the Galaxy

The assumed Galactic gravitational potential has three components namely (i) the disk-halo, (ii) the central bulge, and (iii) the nucleus (Carlberg & Innanen 1987; Kuijken & Gilmore 1959). The potential function for the disk-halo component was assumed to be.

Parameter	disk-halo	nucleus	bulge
Mass($M_\odot$)	1.45 x 10^{11}	9.3 x 10^{11}	1 x 10^{10}
β_1	0.4		
β_2	0.5		
β_3	0.1		
h_1	0.325		
h_2	0.090		
h_3	0.125		
a	2.4		
b	5.5	0.25	1.5

Table 5.1: Parameters of the Galactic potential model.

$$\Phi(R,z) = \frac{-M}{\left[\left\{a + \sum_{i=1}^{i=3} \beta_i \sqrt{z^2 + h_i^2}\right\}^2 + b^2 + R^2\right]^{1/2}} \tag{5.3}$$

the potential function for the other two components was assumed to be,

$$\Phi(R,z) = \frac{-M}{\sqrt{b^2 + z^2 + R^2}} \tag{5.4}$$

Here, R and z are the galactocentric radius and the height from the Galactic plane, respectively. The values of the constants appearing in the above two equations are listed in table 5.1, which has been reproduced from Kuijken & Gilmore (1989). The trajectories are computed with this potential model for time scales as long as 10 Billion years with an accuracy of one part in 100 Million, with adaptive Runge-Kutta method of integration (Press et al. 1992).

5.2.2 Kick speed distributions

As mentioned earlier the velocity of the binary system and hence its position in the Galaxy depends on the asymmetric velocity kick received at the supernova explosion. There is not yet any consensus about the distribution of the kick velocities that neutron stars receive at their birth. We have therefore chosen to explore several different kinds of kick velocity distributions, repeating the full simulation for each assumed kick velocity distribution. Our choice included Maxwellian distributions: $\psi(v_k) \propto v_k^2 \exp(-v_k^2/2\sigma_k^2)$, with $\sigma_k = 50, 100, 150, 200, 300, 500$ km/sec., the distribution proposed by Paczynski (1990): $\psi(v) \propto 1/[1+(v/v_\star)^2]^2$ with $v_\star = 450$ km/sec, and a modified version of it due to Hansen & Phinney (1996) which changes $v_\star$ to 600 km/sec. (we shall refer to this as the Hansen-Phinney-Paczynski (HPP) distribution in the rest of the chapter). In addition, the distribution proposed by Lyne & Lorimer (1993) was also used. For the purpose of comparison we also repeated the synthesis assuming completely spherical mass ejection in the supernova (which implies zero kick velocity).

5.3 The simulation procedure and results

A large number of low mass binaries were generated, with an assumption that they will go through a spiral-in phase during the primary star Roche-lobe overflow. If the initial orbital binding energy was greater than the binding energy of the envelope of the primary star, then the system was omitted. *i.e.,* if the binary coalesces, it is not considered for the simulation. The mass of the helium core of a star was computed with the relation given by Meurs & van den Heuvel (1989).

After the first explosion, the modified semimajor axis and the centre of mass velocity are computed for each surviving binary. With the assumed initial position in the Galaxy, these binaries are evolved in the Galactic gravitational potential for a time, selected (with uniform probability) in the range zero to 10 Billion years.

The initial z-distribution of LMXBs was assumed to be a gaussian with $a =$ 0.075 kpc, and the initial R-distribution was assumed to be uniform in the range

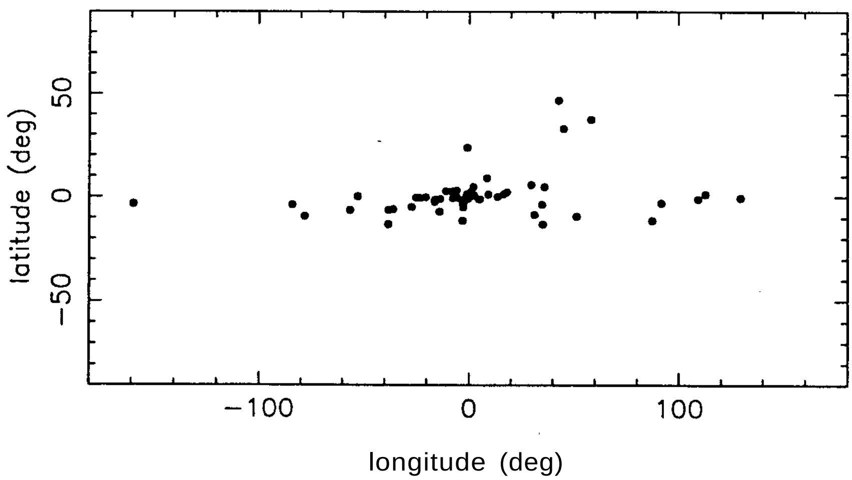

Figure 5.1: The distribution of Low Mass X-Ray Binaries in the Galactic coordinates. Only the LMXBs with confirmed neutron star companions are plotted here (see Paradijs & White 1995).

0 – 15 kpc. However, this is modified to get more realistic distributions in R. by the method of weights described in section 5.3.1

For ever– object, the orbital parameters, along with the initial arid final positions, and velocities were stored.

5.3.1 Comparing simulated LMXBs with known samples

LMXBs derive their space velocities from their centre of mass velocities, which they acquired during the supernova explosion of the primary star. They evolve in the Galactic gravitational potential with this initial velocity. If LMXBs are the progenitors of millisecond pulsars, the kinematic properties of LMXBs must be identical to those of millisecond pulsars. Therefore, the velocities of the simulated LMXBs and millisecond pulsars must be compared with the observed velocities of LMXBs and millisecond pulsars. However, no reliable information on the spatial velocity distribution of LMXBs is available. Therefore, the spatial distribution (Galactic longitude & latitude) of the simulated LMXBs were compared with the observed.

Selecting the known samples

The LMXB catalogue of Paradijs (1995) lists 123 sources. However, the number of LMXBs which are confirmed to have neutron star companions are only a fraction of them. The paper by Paradijs & White (1995) lists 64 such sources. For this simulation, only these sources, with a radio flux cutoff of 10μJy are considered (60 sources). The distribution of these sources as a function of the Galactic coordinates is given in figure 5.1.

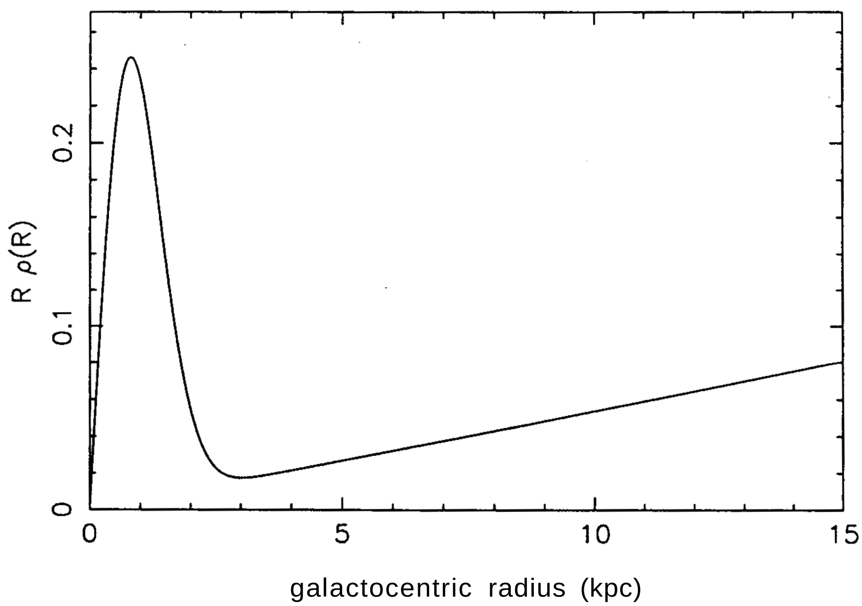

Figure 5.2: The initial galactocentric distribution of LMXBs for which the joint K-S probability was maximum. The central gaussian component has an r.m.s. of 0.8 kpc, and the relative weightage of the flat component with respect to the central gaussian component is **3.8.**

The Method of Weights to compute the initial R-distribution

The comparison of the spatial distribution of the simulated LMXBs with the observed population is not straight forward since one does not know the true initial distribution of LMXBs. Therefore the initial R-distribution of LMXBs was taken as one of the free parameters of the simulation. Though the initial R-distribution was assumed to be uniform in the range of 0 – 15 kpc, weightages were assigned to each object as a function of the initial R value to get the desired distribution, *i.e.*, the simulation was run only once for a given kick speed distribution, and the results were compared with the known samples with various possible initial R-distributions, which were achieved by assigning weights to all the objects depending on their initial Galactocentric radius. The maximum Kolmogorov-Smirnov probability was achieved for a weighting function which has two components: a gaussian, and a flat component (see figure 5.2).

$$W_R = R\left[\frac{1}{\sqrt{2\pi}\sigma}\exp\left(-\frac{R^2}{2\sigma^2}\right)+\frac{w}{225\pi}\right] \tag{5.5}$$

here, a is the r.m.s. of the gaussian component, and w is the relative weightage of the two components. For every asymmetric kick speed distribution, the maximum K-S probability was computed, by varying a and w. To account for the other observational selection effects, another weighting function was used on the basis of distance from the Sun. This weighting function was chosen to be an exponential function $\exp(-d/8.5)$, where d is the distance to the simulated object in kpc.

Various time scales

There are three relevant time scales to this problem. They are, (i) merger time scale due to the emission of gravitational radiation, (ii) tidal synchronisation time scale and (iii) magnetic braking time scale. These time scales are given by the following expressions.

All the binaries in this simulation are assumed to be circular. The merger time scale of these binaries due to the emission of gravitational radiation is given by (Landau & Lifshitz 1975; Taylor & Weisberg 1989),

$$\tau_{\rm GR} = 33701.7\, P_{\rm o}^{8/3} \ \ {\rm Myr} \tag{5.6}$$

here, $P_{\rm o}$ is the initial orbital period in days. The tidal synchronisation time scale $\tau_{\rm syn}$ of the binaries is given by (Tassoul & Tassoul 1992),

$$\tau_{\rm syn} = 5.35 \times 10^{3-N/4} \left(\frac{1+q}{q}\right) \left(\frac{L_\odot}{L}\right)^{1/4} \left(\frac{M}{M_\odot}\right)^{5/4} \left(\frac{R_\odot}{R}\right)^{3} P_{\rm orb}^{11/4} \ \ {\rm years.} \tag{5.7}$$

Here, L, M, and R are the luminosity, mass, and the radius of the star which undergoes tidal distortion, and q is the mass-ratio of the binary system. Here, the orbital period $P_{\rm orb}$ is measured in days. The value of the constant N (which depends on the nature of the envelope of the star) is assumed[1] to be 6. The luminosity and the radius of stars are computed from the stellar evolution models of Schaller et al. (1992).

The magnetic braking time scale is given by (see Verbunt & Zwaan 1981; Verbunt & Hut 1983; Rappaport, Verbunt & Joss 1983),

$$\tau_{\rm mb} = 4.35 \left(\frac{M}{M_\odot}\right) \left(\frac{M_1+M_2}{M_\odot}\right)^{-2} \left(\frac{R_2}{R_\odot}\right)^{-\gamma} \left(\frac{a}{R_\odot}\right)^{5} \ \ {\rm Myr} \tag{5.8}$$

[1]The constant 10^N gives the ratio of the macroscopic to the microscopic viscosities in the envelope of the star. The value of N ranges from zero for radiative envelopes and 10 for convective envelopes. With $N \approx 6 - 10$, the theory by Tassoul & Tassoul (1992) provides the general trend of the observational data, without involving an inordinately large amount of eddy viscosity.

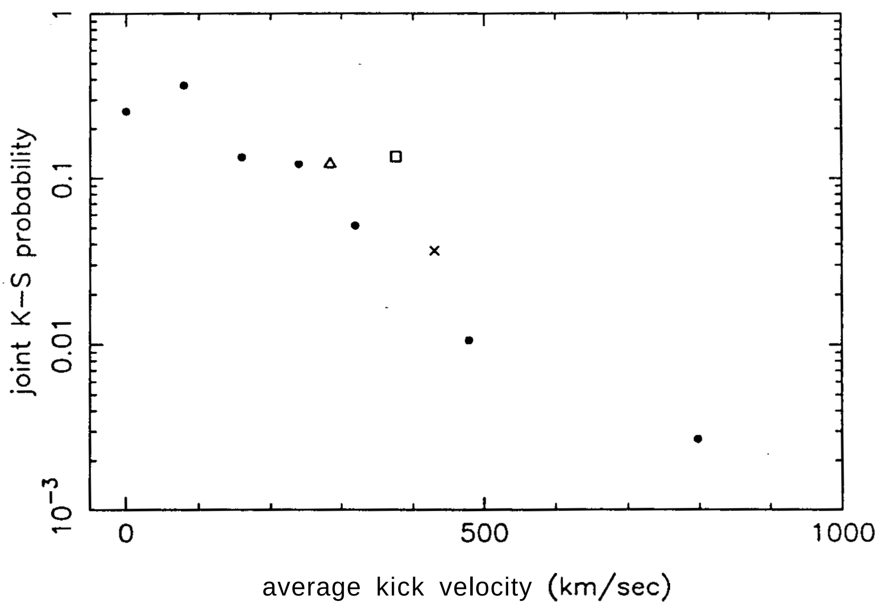

Figure 5.3: The distribution of maximum joint Kolmogorov-Smirnov probabilities for LMXBs as a function of the average speeds of the kick speed distribution. The filled circles indicate Maxwellian kick speed distributions of different σ_k values (average speed of **a** Maxwellian distribution is $\sqrt{8/\pi}$ x σ_k). Lyne & Lorimer, Paczynski and HPP distributions are indicated by cross, triangle and square, with average speeds **430** km/s, 284 km/s and **376** km/s, respectively.

Here, M_1 and M_2 are the masses of primary neutron star and the secondary star respectively. R_2 is the radius of the secondary star, and a is the sernimajor axis of the binary system. The value of γ is assumed[2] to be 2.

A selection criterion was applied on the basis of these three time scales for the simulated set of samples. The criterion was the following. The life time of the binary must be greater than the merger time scale (due to the gravitational radiation), or the maximum of the magnetic braking time scale and the tidal synchronisation time scale. This is because binaries which do not satisfy this criterion may never form a Low Mass X-Ray Binary.

The results of the K-S test, as a function of the kick speed distribution, and the optimum values of a and w are given in table 5.2. Figure 5.3 gives the plot of maximum K-S probability against the average speed of the assumed kick speed distribution.

5.3.2 Comparison of the simulated millisecond pulsar population with the known sample

The spatial distribution of known millisecond pulsars in the Galaxy is severely biased by observational selection effects. If one wants to compare the parameters of the simulated population with the observed, one needs to compensate for all the selection effects. Although one knows in principle how to compensate for the observational selection effects of radio pulsars (Narayan 1987; Narayan & Ostriker 1990), since there are only about a dozen millisecond pulsars for which proper motion is measured one can not do a satisfactory job in compensating for the selection effects. Therefore the following procedure was followed to deal with this problem.

[2] The magnetic braking torque is parametrised with an index γ. According to Rappaport, Verbunt & Joss (1983) $\gamma = 2$ reproduces the orbital period gap in cataclysmic variables well.

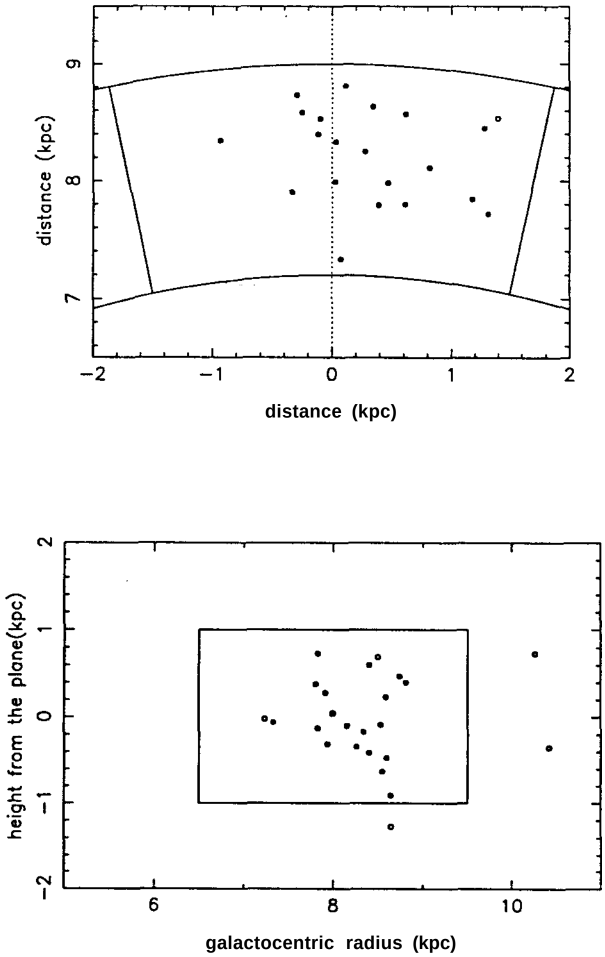

Figure 5.4: The distribution of millisecond pulsars in the Galaxy. The first panel gives the distribution in the Galactic plane, where the Galactic centre is at the origin (0,0), and the Sun is at (0, 8.5). Two arcs are drawn with galactocentric radii of 7.2 kpc and 9 kpc respectively. Two lines are drawn with the azimuth angles (defined in the conventional sense of $\tan^{-1}(Y/X)$) of 78" and 102°. The second panel gives the distribution of millisecond pulsars as a function of the Galactocentric radius and the height from the Galactic plane (z). The box drawn has the limits in z of ± 1 kpc, and in R of 7.2 kpc and 9 kpc. See section **5.3.2** for details.

σ_k (km/sec)	$Q(l)$ x $Q(b)$ (%)	$\psi(R)$ parameters	
		σ_R (kpc)	$\log w$
zero	25.42	0.80	0.58
50	36.70	0.80	0.58
100	13.42	0.80	0.58
150	12.17	0.80	0.49
200	5.17	0.80	0.49
300	1.06	0.80	0.24
500	0.27	0.27	0.41
Lyne & Lorimer	3.65	0.80	0.49
HPP	13.54	0.80	0.58

Table 5.2: The results of the Kolmogorov-Smirnov tests for LMXBs. The first column gives σ_k of the Maxwellian kick speed distributions, and the second column gives the maximum joint K-S probability (for the Galactic longitudes and latitudes). The third and the fourth column give the parameters of the initial Galactocentric radius distribution, for which the K-S probability was maximum. The r.m.s. of the gaussian component is given in the third column, and the relative weightage of the uniform component is given in the fourth.

In the Galactocentric cartesian coordinate system (with the Galactic plane in the X-Y plane), with Sun's coordinates as $(0, 8.5$ kpc$, 0)$, it turns out that almost all observed millisecond pulsars fall in the Galactocentric radius range of $7.2 - 9$ kpc, and in the azimuth angle range (measured upwards from the positive X-axis) of $78^{\circ} - 102^{\circ}$. Moreover, almost all known millisecond pulsars are confined to less than 1 kpc from the Galactic plane. Out of 12 pulsars for which the proper motion measurements exist, 10 pulsars (7 proper motion measurements, and 3 scintillation measurements) fall within this range. Those ten pulsars are, J1857+0943 (Kaspi *et al.* 1994), J1959+2048 (Arzoumanian *et al.* 1994), J2019+2425 (Nice & Taylor 1995), J1300+1240 (Wolszczan 1994), J1713+0747 (Camilo *et al.* 1994), J2322+2057 (Nice & Taylor 1995), J0437-4715 (Bell *et al.* 1995), J1730-2303 (Nicastro & Johnston 1995), J2145-0750 (Nicastro & Johnston 1995), and J1455-

3330 (Nicastro & Johnston 1995). These ten pulsars were considered to describe the transverse velocity distribution of known millisecond pulsars. The simulated LMXBs which fall within the above specified volume (observable volume) were renamed as the observable millisecond pulsars, and only those objects were considered for comparing with the observed sample. The transverse velocities of these objects were compared with the known millisecond pulsars. To compute the transverse velocities of the simulated sample, the azimuth angles of all the simulated objects were reassigned in the range of $78° - 102°$. Then, we computed the transverse velocities with respect to the position of the Sun. The spatial distribution of the known millisecond pulsars is described in figure 5.4. The first panel gives the distribution as a function of the X-Y coordinate system, with the Galactic centre at the origin (Sun is at $x = 0$; $y = 8.5$ kpc). The limits in Galactocentric radius (R) and the azimuth angle are also plotted. The second panel gives the distribution as a function of the Galactocentric radius and the height from the Galactic plane (z). The filled dots indicate the observed millisecond pulsars which fall inside the desired ranges in (R, z, ϕ), and the unfilled circles indicate the objects which fall outside the range.

The Kolmogorov-Smirnov test was used to compare the simulated LMXB population with the observed. However, in the case of millisecond pulsars, K-S test is not a satisfactory test, for there are only 10 objects. Therefore, in addition to the K-S test, another test was performed, which is described below.

The method of "random-pick"

From the set of transverse velocities of the simulated millisecond pulsars, 10 samples are randomly picked. Each of these 10 samples may have different weightages depending on their initial galactocentric radius (see section 5.3.1). The first

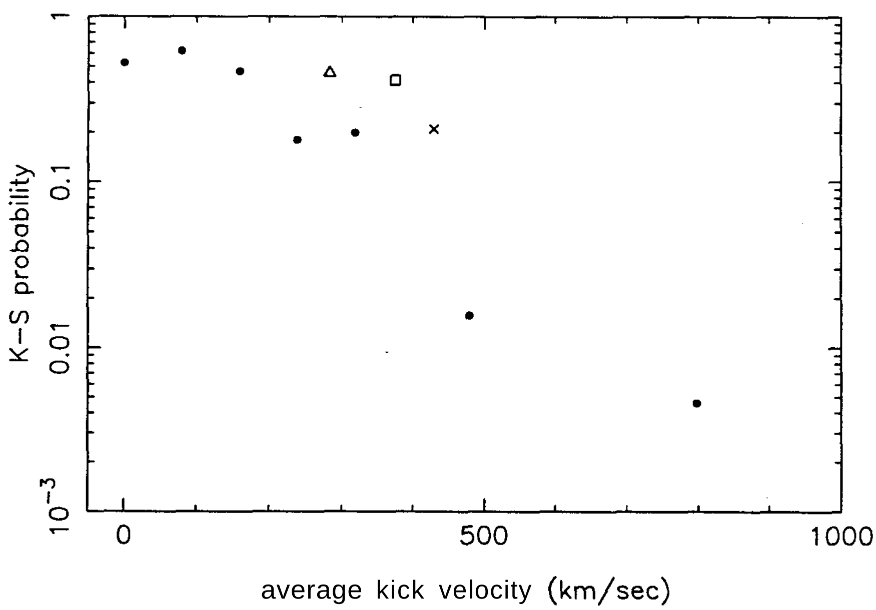

Figure 5.5: The distribution of maximum Kolmogorov-Smirnov probabilities for millisecond pulsars as a function of the average speeds of the kick speed distribution. The filled circles indicate Maxwellian kick speed distributions of different σ_k values (average speed of a Maxwellian distribution is $\sqrt{8/\pi} \times \sigma_k$). Lyne & Lorimer, Paczynski, and HPP speed distributions are indicated by cross, triangle and square, with average speeds 430 km/sec., 284 km/sec. and 376 km/sec., respectively.

moment (average) of these ten samples is computed. This procedure is repeated about 40 thousand times. The location of the average transverse velocity of the known 10 samples with respect to the peak of this distribution of the averages is a measure of the goodness of fit (this may be quantified in terms of the mean and a of this distribution.

Figure 5.5 gives the results of the K-S tests. The maximum K-S probability is plotted against the average speed of the assumed kick speed distribution assumed. Table 5.3 gives the results of the K-S test and the "random-pick" test. In figure 5.6, the mean of the distribution of average transverse velocities (third column of table 5.3) is plotted against the average speed of the assumed kick speed distribution. The error bars are the r.m.s. of this distribution of average transverse velocities (fourth column of table 5.3).

5.4 Discussions and Conclusions

The K-S maximum joint probabilities (see figure **5.3)** ($Q(l)$ x $Q(b)$) for LMXBs indicate that significant probabilities can be achieved for even Maxwellian kick speed distributions with relatively low σ_k values (like zero to 200 km/sec.). Moreover, though the joint K-S probabilities corresponding to Lyne & Lorimer, Paczynski, and HPP distributions are significant, the latter two seem to be marginally better than Lyne & Lorimer distribution.

In the case of millisecond pulsars, the K-S test may not be treated as the best test for there are only ten known pulsars considered for the analysis. However, one must consider the results of the method of "random pick", along with the tesults of the K-S test. Figures 5.5 and 5.6 seem to describe that Maxwellian kick speed distributions with lower σ_k values do equally good job, when compared to the distributions by Lyne & Lorimer, Paczynski, and HPP. However, one can not

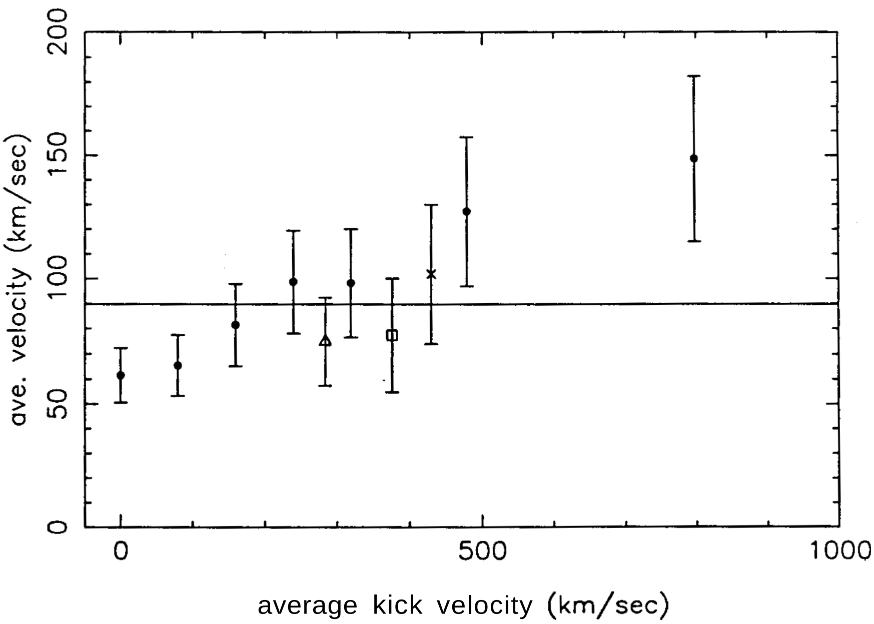

Figure 5.6: The results of the "random pick" method. The horizontal solid line at 89.775 km/sec. is the average transverse velocity of the known millisecond pulsars. The dots indicate the mean of the distribution of averages of randomly picked set of points, as a function of the average speeds of Maxwellian kick speed distributions (average speed is $\sqrt{8/\pi} \times \sigma_k$). The error bar indicate 1 σ deviation of the distribution of averages. Lyne & Lorimer, Paczynski, and HPP distributions are indicated by cross, triangle and square, with average speeds 430 km/sec., 284 km/sec. and 376 km/sec., respectively.

σ_k (km/s)	$Q(V_t)$ (%)	Result of Random Pick	
		$\overline{\langle V_t \rangle}$ (km/s)	$\sigma_{\langle V_t \rangle}$(km/s)
zero	52.59	61.4	10.9
50	61.92	65.4	12.1
100	46.70	81.5	16.4
150	17.93	98.8	20.7
200	19.77	98.4	21.8
300	1.57	127.3	30.2
500	0.46	148.6	33.6
Lyne & Lorimer	20.88	102.0	28.1
HPP	45.44	75.0	17.6

Table 5.3: Comparison of simulated millisecond pulsars with observed population. As mentioned in section 5.3.2 the LMXBs which fall in some specified range of the Galactocentric coordinates are renamed as observable millisecond pulsars. The first column of this table gives σ_k of the kick speed distribution, and the second column gives the maximum Kolmogorov-Smirnov probabilities for the transverse velocity distribution of the simulated population to be the same as that of the observed. The third and the fourth columns give the results of the "random-pick" method. The average of the distribution of average transverse velocities is given in the third column, and the r.m.s. is given in the fourth column. (for details, refer to section 5.3.2).

rule out these distributions with the present set of known sample.

When the results of LMXBs and millisecond pulsars are compared with each other, they seem to agree well, within the errors. This lends support to the hypothesis that LMXBs are the progenitors of millisecond pulsars.

Figure 5.7 gives the centre of mass speed distributions of binary systems, just after the primary supernova explosion. Figure 5.8 gives the speed distribution in the "observable" volume of millisecond pulsars ($7.2 \leq R \leq 9$ kpc, $|z| \leq 1$ kpc) after evolving in the galactic potential for upto an age of 10 Byr. The solid curves correspond to σ_k of zero. 100, 200 and 300 km/sec. (from the narrowest to the broadest). The 'dotted' curve corresponds to the Lyne & Lorimer distribution.

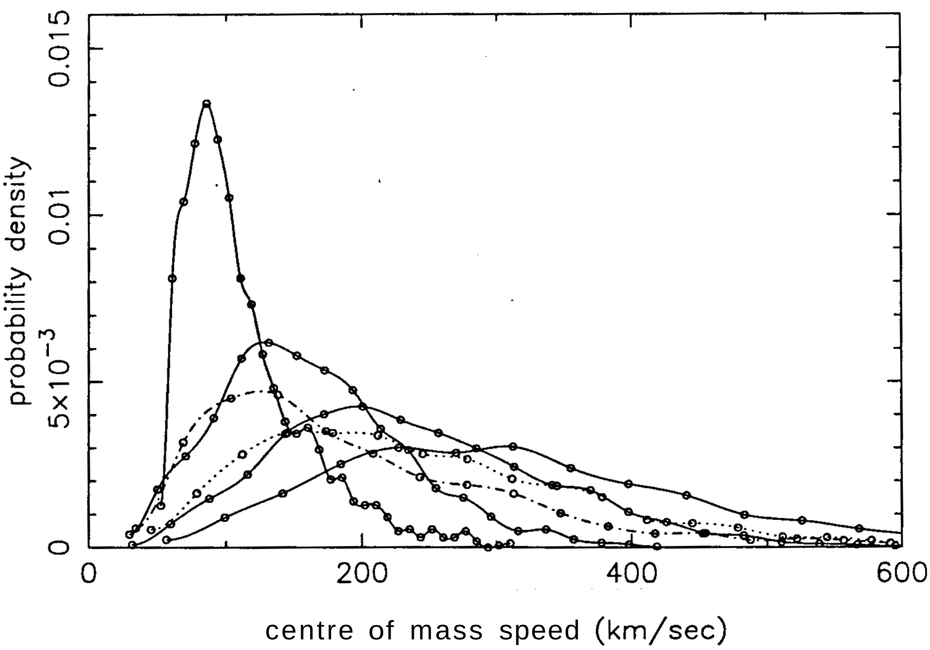

Figure 5.7: The centre of mass speed distribution of Binaries just after the supernova explosion. The solid lines indicate the distributions corresponding to the input Maxwellian kick speed distributions with σ_k of zero, 100, 200, and 300 km/sec. (from the narrowest to the broadest). The 'dotted' line indicates the distribution for Lyne & Lorimer distribution, and the 'dash' line indicates the distribution for HPP distribution.

and the 'dash-dot' curve corresponds to the HPP distribution. As can be seen, the distributions in figure 5.8 differ significantly from the corresponding distributions in figure 5.7. The reason for this difference is two fold. The evolution in the Galactic potential for ages upto 10 Byr modifies the distributions significantly, and the high velocity objects can easily escape from the "observable" volume, leaving behind only the lower velocity objects. This would suggest that the velocities of observable millisecond pulsars are, on the average, much lower than that of ordinary pulsars, whose average velocity is modelled to be greater than 400 km/sec (Lyne & Lorimer 1993; Hansen & Phinney 1996).

The three time scales described in section 5.3.1 help us to neglect the binary systems which may not end up in producing LMXBs for they may coalesce due to various angular momentum loss mechanisms (see Kalogera & Webbink 1996).

The subject discussed in this chapter has been investigated by others too (Paradijs & White 1995; Brandt & Podsiadlowski 1995). The procedure followed in this chapter is, however, more detailed and complete. The results of Paradijs & White suggests than the distribution of Lyne & Lorimer fits well with the observed LMXBs. The difference between our results and the result of Paradijs & White may arise due to the reason that they have not treated the evolution of LMXBs in the full three dimensional gravitational potential of the Galaxy. The results derived by evolving the bodies in the full potential may differ significantly from the results derived on the basis of the local potential, for the local potential tends to under estimate the scale height.

The main difference between the work described in this chapter and of Brandt & Podsiadlowski (1995) are the following. The initial distribution of binaries as a function of the galactocentric radius was taken as a free parameter in our simulation, where as in their work, it was assumed to be an exponential distribution.

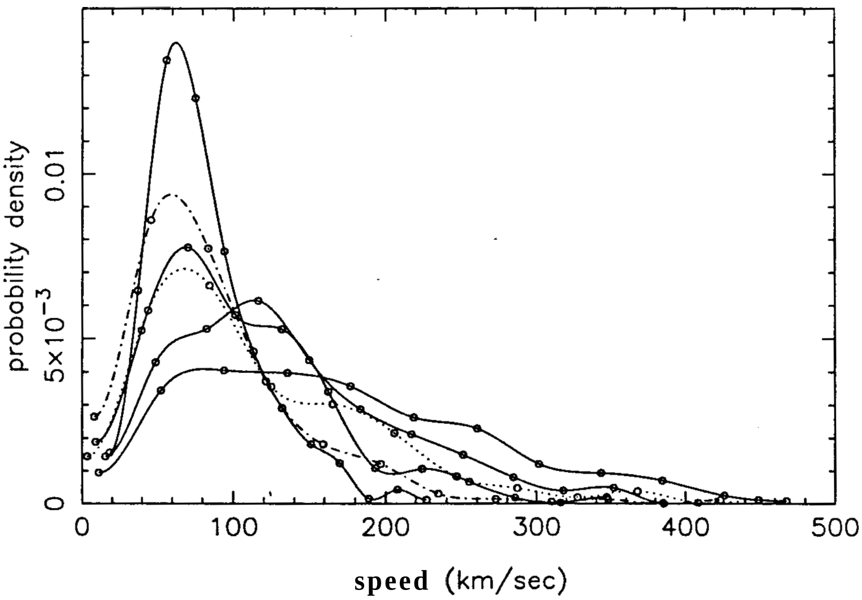

Figure 5.8: The speed distribution of millisecond pulsars. The solid lines indicate the distributions corresponding to the input Maxwellian kick speed distributions with σ_k of zero, 100, 200, and 300 km/sec. (from the narrowest to the broadest). The 'dotted' line indicates the distribution for Lyne & Lorimer distribution, and the 'dash' line indicates the distribution for HPP distribution.

While comparing the simulated set of LMXBs with the observed, the whole distribution (in galactic latitudes and longitudes) was considered, unlike the work of Brandt & Podsiadlowski (1995) where they have considered (cos8) and (sin b), where 8 is the angle between the object and the Galactic centre, and b is the latitude of the object. Their conclusion that the velocity distribution of Lyne & Lorimer (1993) fits well with the observed sample set is not inconsistent with our conclusions. However, we have considered many number of distributions (Maxwellians of different σ_k values, Lyne & Lorimer distribution, HPP distribution etc.).

The main conclusions of this chapter can be listed as follows.

- The kinematic properties of LMXBs and millisecond pulsars are consistent with each other, and it supports the idea that LMXBs are the progenitors of millisecond pulsars.

- Though the results of Lyne & Lorimer speed distribution seems to agree with the observations, the HPP distribution and Maxwellians with significant number low speed pulsars seem to be better.

- The average speed of millisecond pulsars seems to be considerably lower than that of the normal pulsars.